UNIVERSITY OF CALIFORNIA, SAN DIEGO
SCRIPPS INSTITUTION OF OCEANOGRAPHY
VISIBILITY LABORATORY
SAN DIEGO, CALIFORNIA 92152

AN APPARATUS FOR THE MEASUREMENT OF AN EFFECT OF ATMOSPHERIC BOIL
(The Shimmer Meter)

S. Q. Duntley, J. L. Harris, R. W. Austin

SIO Ref. 68-15
July 1968

Naval Ship Systems Command
Contract NObs-84075
Assignment 9
Final Report

Approved:

S. Q. Duntley

Seibert Q. Duntley, Director
Visibility Laboratory

Approved for Distribution:

William A. Nierenberg

William A. Nierenberg, Director
Scripps Institution of Oceanography

Fig. 1. Shimmer Meter

FOREWORD

This report describes many previously unpublished details concerning an instrument which was constructed, used briefly, and dismantled during 1957. The device was for the measurement of the blurring of fine details by atmospheric boil in the case of images formed by telescopic or photographic objectives of long focal length. A recent resurgence of interest in this topic has resulted from current research on the restoration of atmospherically distorted images by means of image processing. This has prompted certain former work on effects due to atmospheric boil to be reviewed.

Most of this report has been lifted almost verbatim from internal memoranda or letters written in 1957. Almost no effort has been made to update the concepts expressed in those writings. Thus, with minor exceptions, the report is exactly as it might have been issued in 1957. The concepts contained in the sections entitled "INTRODUCTION AND SUMMARY" and "THE NATURE OF ATMOSPHERIC BOIL" (except for the short subsection called "Soft Shimmer and Hard Shimmer") do not conform completely with those held by the authors in 1968, but it has been decided to issue these sections just as they were written in 1957 because in no other way can the background against which the "shimmer meter" was conceived, designed, and used be made clear.

The work described by this report was performed in 1957 under Bureau of Ships contract NObs-72092. The report has been prepared and issued as the final report under assignment 9 of contract NObs-84075.

INTRODUCTION AND SUMMARY

The resolution of fine detail in high-flying objects when photographed by tracking cameras of long focal length as well as the resolution achievable by astronomical telescopes when used for planetary and stellar photography is often limited by atmospheric boil. Optimization of the performance of telescopes and tracking cameras requires a quantitative measure of the deleterious effect of atmospheric boil, particularly on the higher spatial frequency content of the image.

This report presents a method for the measurement of an effect of atmospheric boil in terms of the root-mean square deviation of the image-forming rays that contribute to the reproduction of fine detail, and describes an experimental (breadboard) version of an instrument employing this method. A sample of data obtained with the instrument near Cape Kennedy, Florida is presented.

In Appendix A of this report the effect of refractive inhomogeneities in the atmosphere (boil) on image quality is described in terms of the variance of a two-dimensional normal distribution describing the frequency of the apparent angular position of object points. The shimmer meter measures the temporal average of this variance throughout any arbitrary time interval by sensing the temporal variations in the shape of an image of a planet, the moon, or the sun as observed by a photo-electric cell through a narrow slit protruding radially beyond the edge of the image. The variance, time-averaged over any interval T, can be read from any highly damped, true mean-square indicator provided the

current output of the photoelectric cell is passed through a filter having an amplitude characteristic $\left[1 - \sin^2 1/2\lambda T/(1/2\lambda T)^2\right]^{\frac{1}{2}}$. The variance which characterizes any other path of sight can be found by multiplying the measured variance by the ratio of the secants of the respective zenith angles. Multiple slits can be used to minimize vibration and tracking effects. Data with this equipment illustrate how photographs can be improved by using short exposures and optimum aperture size.

THE NATURE OF ATMOSPHERIC BOIL

Astronomers and others have long known that "seeing" is impaired by the existence within the atmosphere of small volumes of air differing slightly in refractive index from that of their surroundings. These refractive parcels or turbulence range in size from that of a man's head to tiny volumes the size of bird-shot. They represent thermal microinhomogeneities within the atmosphere; they may also reflect inhomogeneities in water vapor distribution. In any case, they are found near heat sources such as the ground, chimneys, engine exhausts, etc. At night the occurrence of parcels is reduced in comparison with normal daytime conditions and they are larger.

Visual Examination of Parcels

Astronomers can see individual parcels drifting across the opening of their telescope by inserting a pinhole stop in the image plane of their objective so that only light from a single bright star is admitted and then adjusting the eyepiece system to provide a Maxwellian view

(i.e., image the star on the pupil of the eye rather than on the retina). The entrance pupil of the telescope is then imaged on the retina and this image is in terms of light of extremely high collimation. Under these circumstances slight refractive deviations caused by the parcels make part or all of the deviated light miss the pinhole stop so that the parcels are visible as dark areas on the otherwise bright lens aperture. Under favorable nighttime seeing conditions, large parcels several inches in diameter are seen to drift slowly across the telescope aperture. Under less favorable conditions a complex, restless pattern appears as the result of multiple parcels, often of small size, distributed in depth along the path of sight.

Normal Astronomical Photography

A stellar image formed by a telescope objective large enough to encompass many parcels will consist of the superposition of many slightly displaced star images. The photograph will then consist of a blurred image and even (occasionally), for short exposure durations, multiple images. If the telescope is stopped down until a single parcel can fill the entire aperture, the star image will move about the film plane as nearby parcels drift across the lens and change in apparent intensity (scintillate) in response to the movement of more distant ones. Motion picture recordings with short exposure duration exhibit these behaviors but individual frames show comparatively sharp images. If the exposure duration is lengthened, the resulting photograph shows a blur pattern which represents a time-average of the wandering image. In the limit, the time-averaged blur pattern from a small objective and the space-averaged blur pattern from an entrance pupil very large compared with

the parcel size are somewhat similar.

Effect of Parcel Distance

Refractive parcels close to the telescope lens produce image motion and blurring as described above, but virtually all of the light is collected by the objective lens regardless of the magnitude of the deviation produced by the nearby parcel. In the case of distant parcels, however, the deviated light may miss the telescope lens entirely. Thus, the distant parcels may produce a temporal modulation in the total flux collected by the telescope in addition to blurring and time-varying distortion effects. Thus stars are observed to twinkle on a night when poor seeing is caused by the presence of refractive parcels at high altitudes.

Normal Night Conditions

Under mild nighttime seeing conditions a photoelectric telephotometer having a field of half a degree mounted ten feet above brush covered terrain and aimed horizontally at a bare lamp located a mile distant may show a four-fold temporal flux modulation. Virtually all frequencies are present from fractional cycle changes up to the middle audio range, but there is often a strong peak centering around four cycles per second. This is responsible for the appearance of rapid twinkle or "scintillation."

In visual observations all frequencies above about 15 cycles will be time-averaged by the eye, resulting in blurring. Temporal integration by a camera depends, obviously, on exposure time. Lens diameter may have less effect on the contributions of distant parcels than on the

effects due to parcels close to the objective.

In addition to the flux modulation, distant parcels cause image wander and multiple image formation. Most of the observed deviations are probably the result of many small deviations due to the passage of light through parcel after parcel along the path of the ray. Parcels sometimes occur in layers which move at different velocities. Strange appearing effects may result, such as the illusion of waves of shimmering air drifting opposite to the direction of the wind.

Day Conditions

Day conditions are, obviously, of concern in the operation of tracking cameras. The effects caused by refractive parcels increase after sunrise and may become severe during the middle of the day. The parcels become smaller and their motions due to convection become more rapid as the ground grows warmer. There is, therefore, greater emphasis on the higher temporal frequencies, resulting in greater temporal integration both visually and photographically. Thus, resolution is decreased.

The refractive deviations remain quite small, however, rarely exceeding a minute of arc. Naked eye resolving power and the resolution of short focal-length cameras are, therefore, not appreciably affected, although the larger, slower deviations are seen as distortion and "shimmer." The resolving power of telescopic visual systems and of long focal-length cameras, however, is markedly reduced and it is a rare day when systems inherently capable of resolving a second of arc are able to do so along horizontal paths of sight close to the ground.

Effect of Elevation

Refractive parcels are often most numerous close to the ground. Improvement is so rapid with altitude that there is rich reward in elevating the horizontal path of sight even a few feet. In the case of upward paths of sight the air near the ground is usually the principal offender. Camera elevation results in marked improvement provided that tne instrument itself or its elevated mound does not give rise to excessive parcel production.

Jet Exhausts and Chimneys

An interesting illustration of resolving power loss due to refractive parcels is furnished by every jet take-off. Any observer standing near the runway and looking horizontally through the mass of hot, turbulent gases left by the jet will observe a marked reduction in resolving power and, moreover, a marked loss in the apparent contrast of objects seen against uniform backgrounds such as the horizon sky. Another example of the same phenomenon is found at the top of every chimney giving forth hot gases free of smoke. Experiments on the output of chimneys show that the parcel size is very small, resembling bird-shot. The root-mean-square diameter of the refractive parcels in a jet exhaust is, doubtless, in the sub-millimeter range. Under such conditions short exposure cannot be expected to produce sharp images. Blurring will also be observed because every path of sight must traverse many, many tiny refractive parcels.

Soft Shimmer and Hard Shimmer

Astronomers have used the terms soft shimmer and hard shimmer to designate the two limiting cases of effects that have been described in the preceding paragraphs. Thus, when images are blurred regardless of how short an exposure interval may be used in recording them, a state of soft shimmer is said to prevail, but when sufficiently short exposures result in sharp but distorted images, the shimmer is said to be hard. Not infrequently both soft and hard shimmer effects appear in the same photograph of an extended object. Fourier analysis of the structure of images shows that the higher spatial frequencies in an image are produced by the extremities of the entrance pupil of the telescope and are determined by the phase distortion associated with these small areas. The phase of the low frequency components of the image is determined, however, by an average over a large portion of the entrance pupil. The highest spatial frequency passed by the optical system is associated with two extreme points on the entrance pupil. This highest frequency will be affected by the time-varying phase of the light at these points. Thus in any telescopic system, regardless of its size, a short exposure will result in hard shimmer for the highest spatial frequencies even though the lower frequencies may be in a state of soft shimmer. The shimmer meter described in this report makes use of this fact.

See James L. Harris, "Restoration of Atmospherically Distorted Images," Scripps Institution of Oceanography Reference 63-10 (March 1963), Sec. 6, pp. 21-28.

QUANTITATIVE RELATIONS

Appendix A of this report is a reprint of a paper entitled "Reduction of Contrast by Atmospheric Boil" in which equations are developed for the time-averaged radiance distributions observable by a camera when looking at objects of circular, square, rectangular, and other shapes seen against a uniform background such as the sky. In deriving these equations, use is made of random-walk statistics to develop the theorem that the time-averaged blur pattern from any point of the object is Gaussian and describable by a variance or mean-square deviation for the rays which form the fine details of the object. Thus, as shown on page 357 of Appendix A, the time-averaged absolute apparent contrast $\bar{C}_r(z,\theta,\phi)$ at the center of a uniform circular object having an angular radius ψ and an absolute apparent contrast $C_r(z,\theta,\phi)$[1] in the absence of shimmer is:

$$\bar{C}_r(z,\theta,\phi) = C_r(z,\theta,\phi)\left(1 - e^{-\frac{1}{2}\left[\psi^2/Ar\right]}\right). \tag{1}$$

By replacing the product Ar with the path variance $\left[\sigma_r(z,\theta,\phi)\right]^2$ and considering the case of an object outside the atmosphere of the earth, Eq. (1) can be written:

$$\bar{C}_\infty(z,\theta,\phi) = C_\infty(z,\theta,\phi)\left(1 - e^{-\frac{1}{2}\left[\psi/\sigma_\infty(z,\theta,\phi)\right]^2}\right). \tag{2}$$

---

[1] The notation $C_r(z,\theta,\phi)$ denotes the apparent contrast of an object at distance r from an observer at altitude z looking along a path of sight having a zenith angle θ, and an azimuth angle ϕ. Correspondingly, $\left[\sigma_r(z,\theta,\phi)\right]^2$ refers to the variance of a path of sight of length r terminating at altitude z and having zenith angle θ and azimuth angle ϕ.

THE SHIMMER METER

Any means for measuring the path variance $\left[\sigma_{\infty}(z,\theta,\phi)\right]^2$ or the root-mean-square deviation $\sigma_{\infty}(z,\theta,\phi)$ for those image-forming rays which control the higher spatial frequencies in the image provides the necessary datum for calculating the time-averaged apparent contrast of small distant objects by means of the equations given in Appendix A.

The shimmer meter was devised as a means for measuring $\sigma_{\infty}(z,\theta,\phi)$ for the total atmospheric path between an object outside the earth's atmosphere and the observing station. This was accomplished by observing the temporal distortions of the image of the sun. An image of the moon, a planet, or any extended object in space can be used in the same way.[2] If the atmosphere is horizontally homogeneous and azimuthally isotropic with respect to its boil properties, the ratio of the path variance $\left[\sigma_{\infty}(z,\theta,\phi)\right]^2$ in the direction of the object to the path variance $\left[\sigma_{\infty}(z,\theta_s,\phi_s)\right]^2$ in the direction of sun (moon, planet, etc.) equals the ratio of the respective path lengths or

$$\frac{\left[\sigma_{\infty}(z,\theta,\phi)\right]^2}{\left[\sigma_{\infty}(z,\theta_s,\phi_s)\right]^2} = \frac{\sec\theta}{\sec\theta_s} ,$$

if effects due to earth curvature are negligible.

An experimental version of the shimmer meter, shown in Fig. 1, was assembled from borrowed and available components and operated briefly at Patrick Air Force Base, Florida during the spring of 1957. It

---

[2] A shimmer meter like that described and pictured in this report can be used to measure the path variance (i.e., the product Ar) along terrestrial paths of sight (horizontal or inclined) by aiming it at a bright circular object of the proper angular size; e.g., the exit pupil of a projector located at some known distance r could be used. Data obtained with such a terrestrial shimmer meter would enable long-range terrestrial photography to be optimized for the prevailing conditions and, by means of Appendix A, should enable the results of such pictures to be better interpreted.

was subsequently dismantled. The optical system of that instrument is shown schematically in Fig. 2 and a photograph of it appears as a frontispiece (Fig. 1) of this report. An image of the sun was formed on a pattern of slits behind which was a multiplier phototube. An available astronomical objective 6 inches in diameter and 100 inches in focal length was mounted in an internally blackened and baffled metal tube and attached to an available crude but rugged equatorial tripod mounting which carried an aiming telescope. The sun was tracked manually by means of a hand-operated tangent screw, which is not visible in Fig. 1. The front surface of the telescope objective was given a nearly opaque aluminum coating in order to reflect most of the incident sunlight and, thereby, avoid heating of the internal parts of the shimmer meter and the air within its tubing. An adjustable iris diaphragm was mounted in front of the objective lens in order to provide an easy means for altering the diameter of the entrance pupil of the system. The solar image was formed on a metal plate containing the pattern of four radial slits shown in Fig. 3. The only light able to reach the cathode of the multiplier phototube passed through these slits.

Only a single radial slit would have been used in the shimmer meter if the instrument could have tracked the sun perfectly; the four-slit pattern was adopted only to render the readings of the shimmer meter immune to tracking imperfections, including vibration of the mount. For simplicity, consider first the case of perfect tracking. The slit plate would then appear as in Fig. 4, with the solar image filling half the slit. Atmospheric boil would then cause the image of the limb of the sun to move left and right, thereby modulating the flux transmitted by

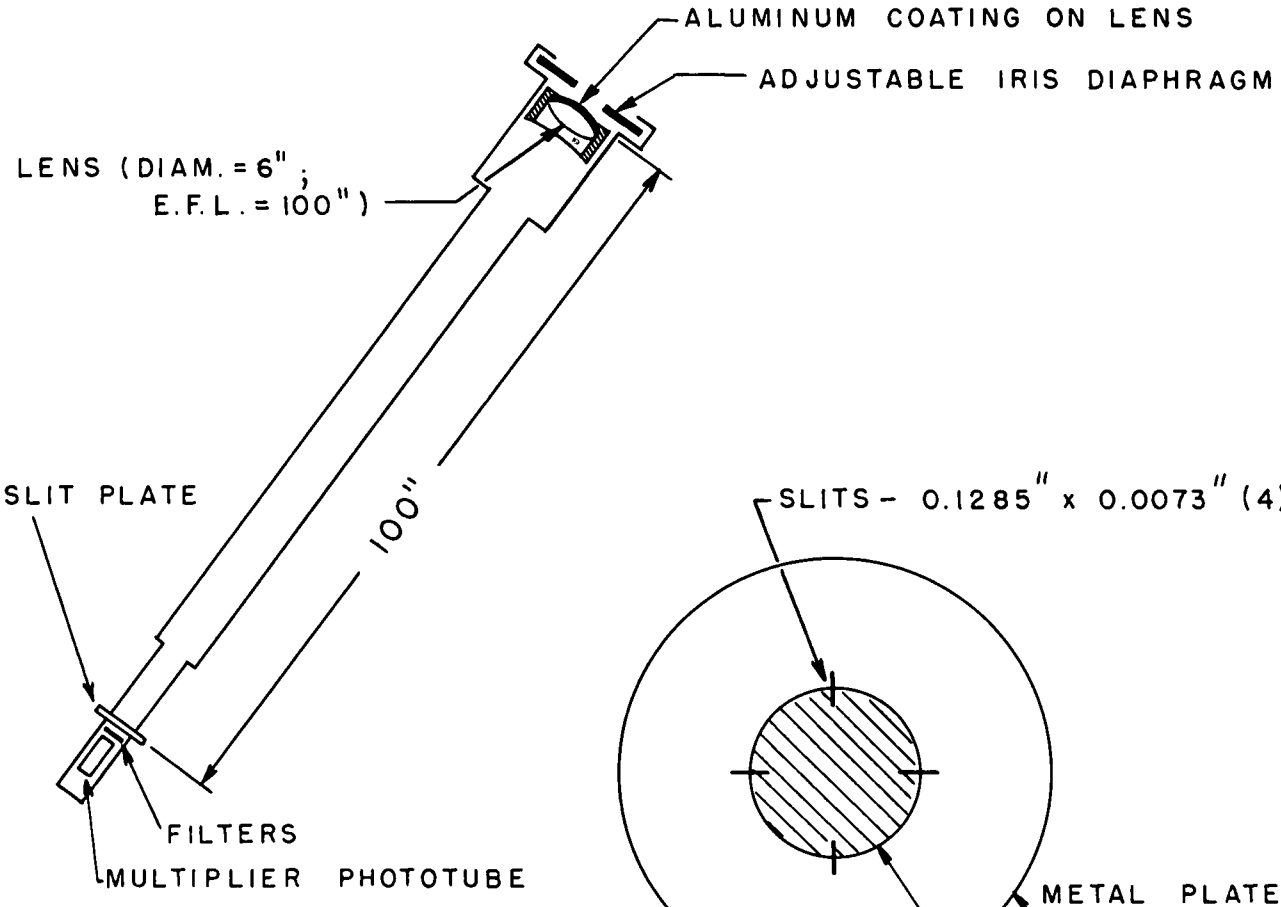

Fig. 2 - SHIMMER METER

Fig. 3 - SLIT PLATE (FOUR SLITS)
(FULL SIZE)

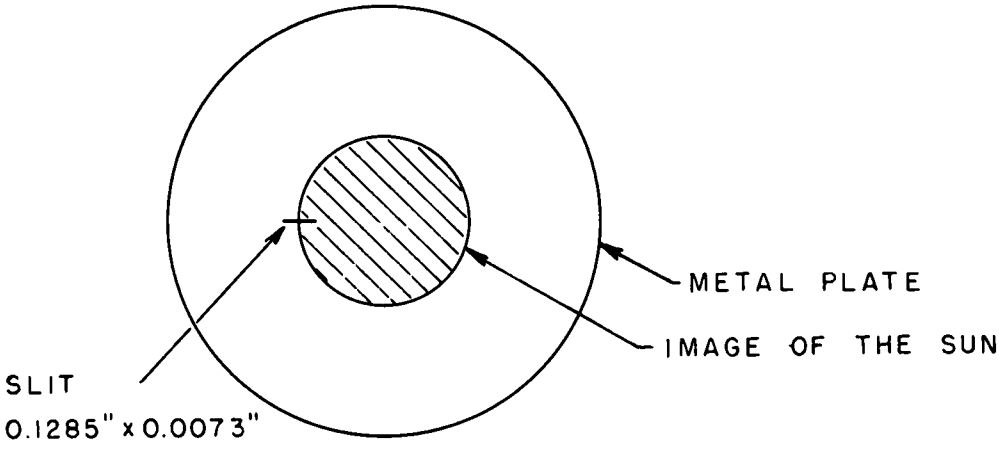

Fig. 4 - SLIT PLATE (ONE SLIT)
(FULL SIZE)

the slit.* The photoelectric photometer measures the modulation of the flux transmitted by the slit.

Appendix B shows that it is essential for the interpretation of shimmer meter readings that the motion of the solar limb be almost completely correlated across the width of the slit. Experiments on time-varying characteristics of optical transmission through atmospheric boil have been described by Riggs, Mueller, Graham, and Mote,[1] who found that for a horizontal path length of several hundred meters the instantaneous displacement of points separated by one-half minute of arc were 50 per cent correlated, whereas those of points separated by more than 5 minutes of arc were uncorrelated. Based upon the curves published by Riggs, Mueller, Graham, and Mote, the slits of the shimmer meter were made 1/4 minute of arc in width (i.e., 0.00727 inches) in the belief that the average correlation of the solar image within slits of this width is greater than 80 per cent. Light from the sun is so plentiful that even finer slits could have been used, and an even greater degree of correlation obtained.

In the absence of tracking errors, the length of the slit could and should be made short enough to cause the atmospheric displacements of the image of the solar limb to produce a high percentage of modulation, thereby relaxing the requirements to be met by the electronic system. In the case of the experimental shimmer meter, however, the tangent-screw tracking left much to be desired and the mounting, although

---

[1] Riggs, Mueller, Graham, and Mote, J. Opt. Soc. Am. 37, 415(1947).

*The solar image also moves up and down in Fig. 4 but this component of motion is negligible because of the narrowness of the slit.

rugged by ordinary standards, did undergo small oscillations whenever wind was present. Although these tracking defects were eliminated by the use of the four-slit pattern shown in Fig. 3, it was necessary, nevertheless, to make the slits long enough to insure that the solar image would never come to the end of the slit. The slits in the only slit plate ever prepared were 0.1285 inches in length, corresponding to 265 seconds of arc. Thus, the slits were nearly 18 times as long as their width. Although the percentage modulation of the photocell current was often considerably less than 1 per cent when these long slits were used, the electrical system had no difficulty in successfully dealing with this signal input and, during the short course of the experiments, no other slit plate was made.

The shimmer meter would have been hopelessly inoperative because of the manual tracking errors if only a single slit had been used. The four-slit pattern, however, shown in Fig. 3, eliminated the effect of manual tracking faults by making the effective fractional length of the slit filled by solar image always one-half. This was important since it established the dc level against which the modulation was measured.

Because the angular diameter of the sun is approximately 30 minutes, the electrical modulation components due to each of the four slits were completely uncorrelated. They combined, therefore, in the manner of random events so that the signal-to-noise ratio of the four-slit shimmer meter was less by a factor of $\sqrt{4}$ than that which would have resulted from the use of a single slit, assuming the average flux to have been adjusted to a selected level. This trivial penalty was accepted in order to obtain the vitally needed freedom from vibration and tracking defects.

The Electronic System of the Shimmer Meter

The electronic system of the shimmer meter, in addition to the multiplier phototube, consisted of a single electronic package and a thermal voltmeter. These units are shown in Fig. 5. The only controls requiring attention by the operator were the two rotary switches which appear as black knobs in the photograph. The right rotary switch controlled the electrical filter and was marked in terms of equivalent photographic exposure duration, the positions of the switch being marked respectively, 1/10th, 1/50th, 1/100th, 1/250th, 1/500th, and 1/1000th second.

The rotary switch at the left was an attenuator which controlled the gain of the amplifier. Its positions corresponded with amplifier gains of 100, 50, 20, and 10. The circuit employed is shown in Fig. 6. In the upper right-hand corner of this figure is shown the multiplier phototube which, together with its 6AV6 cathode follower, was mounted behind the slit plate in the shimmer meter (see Figs. 1 and 2). A cable connected the output of this cathode follower to the chassis shown in Fig. 5. This contained a high voltage supply and a control circuit of the Sweet[2] type designed to operate the multiplier phototube at a voltage such that its anode current was nearly independent of light level insofar as slow variations in light were concerned. This was an important feature because, as a modulation meter, constant dc current level is essential to direct-reading operation. The success with which current constancy was achieved was demonstrated whenever thin wisps of cloud passed across the sun. These clouds were sufficiently tenuous that the solar disk was always visible, but they were dense enough to

---

M. H. Sweet, J. Soc. Motion Picture Engineers 24, 35(1950).

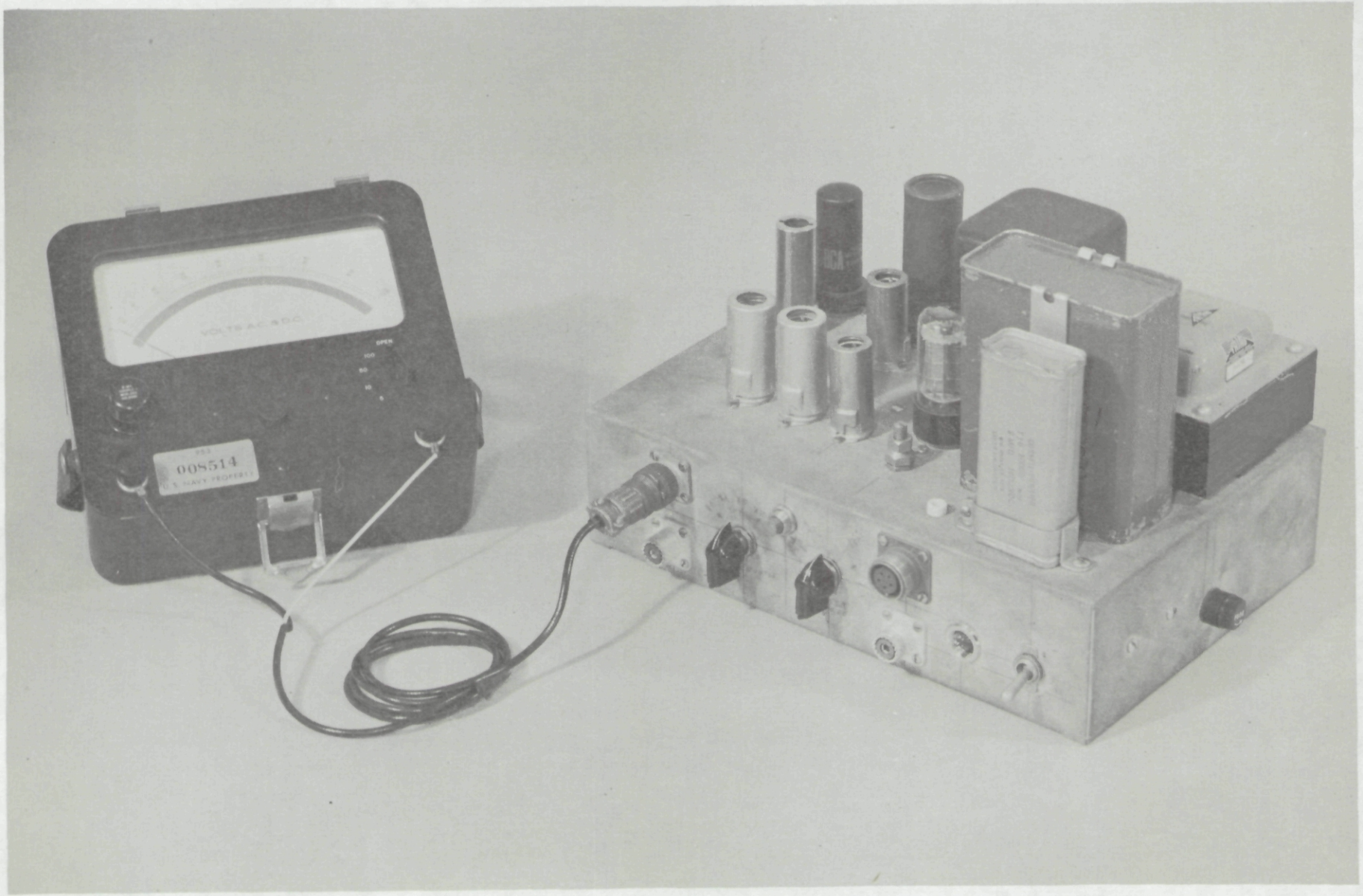

Fig. 5

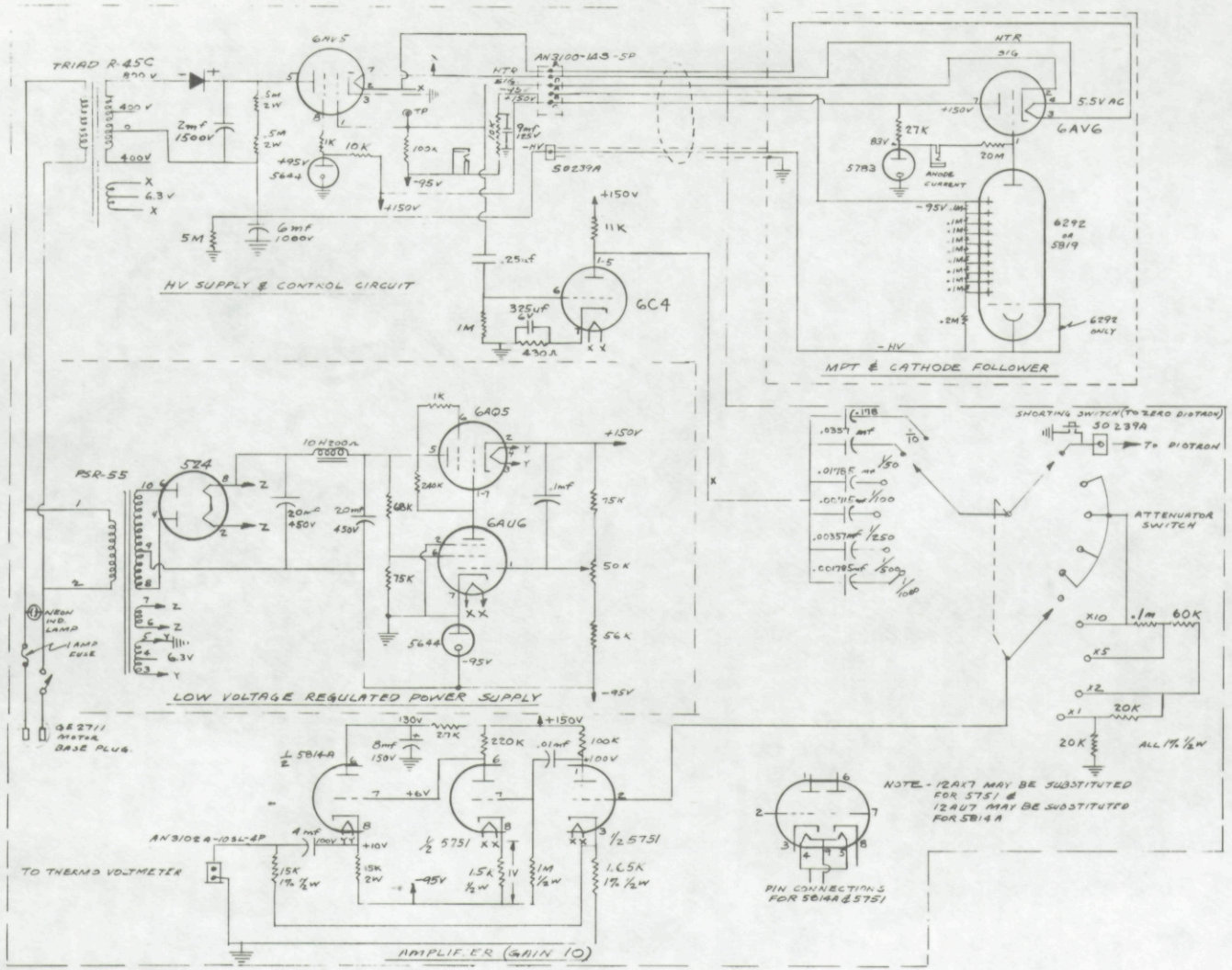

Fig. 6. Circuit Diagram

make a considerable variation in the light level on the photocathode. No effect on the output of the shimmer meter could be detected due to the passage of such clouds.

Because the modulation produced at the slits was small, making amplification of the signal necessary, circuit induced noise was always present in the output, and readings were easiest to make with a highly damped instrument, such as a thermal voltmeter. It was important, moreover, that the readout device measure the true root-mean-square value of the electrical waveform, and no meter performs this function better within its frequency range than a thermal instrument for this application. In practice, the thermal meter was operated in its most sensitive mode and the readings were kept on scale by means of the internal attenuator in the shimmer meter electronic chassis.

Filtering of the Shimmer Meter

This subject is discussed in detail in Appendix B of this report, wherein it is shown that the output of the modulation meter must be measured after weighting its frequency content with a filter having an amplitude characteristic $\left[1 - \sin^2 \frac{1}{2}\pi/(\frac{1}{2}\pi T)^2\right]^{\frac{1}{2}}$.

It is also demonstrated in Appendix B that a filter having the required characteristic can be approximated by means of a simple RC network, and such a network was provided in the shimmer meter, as shown at the right in Fig. 6. The measured response of the system in each of the positions provided by the rotary switch is shown in Fig. 7. The equivalent exposure interval I associated with each position of the

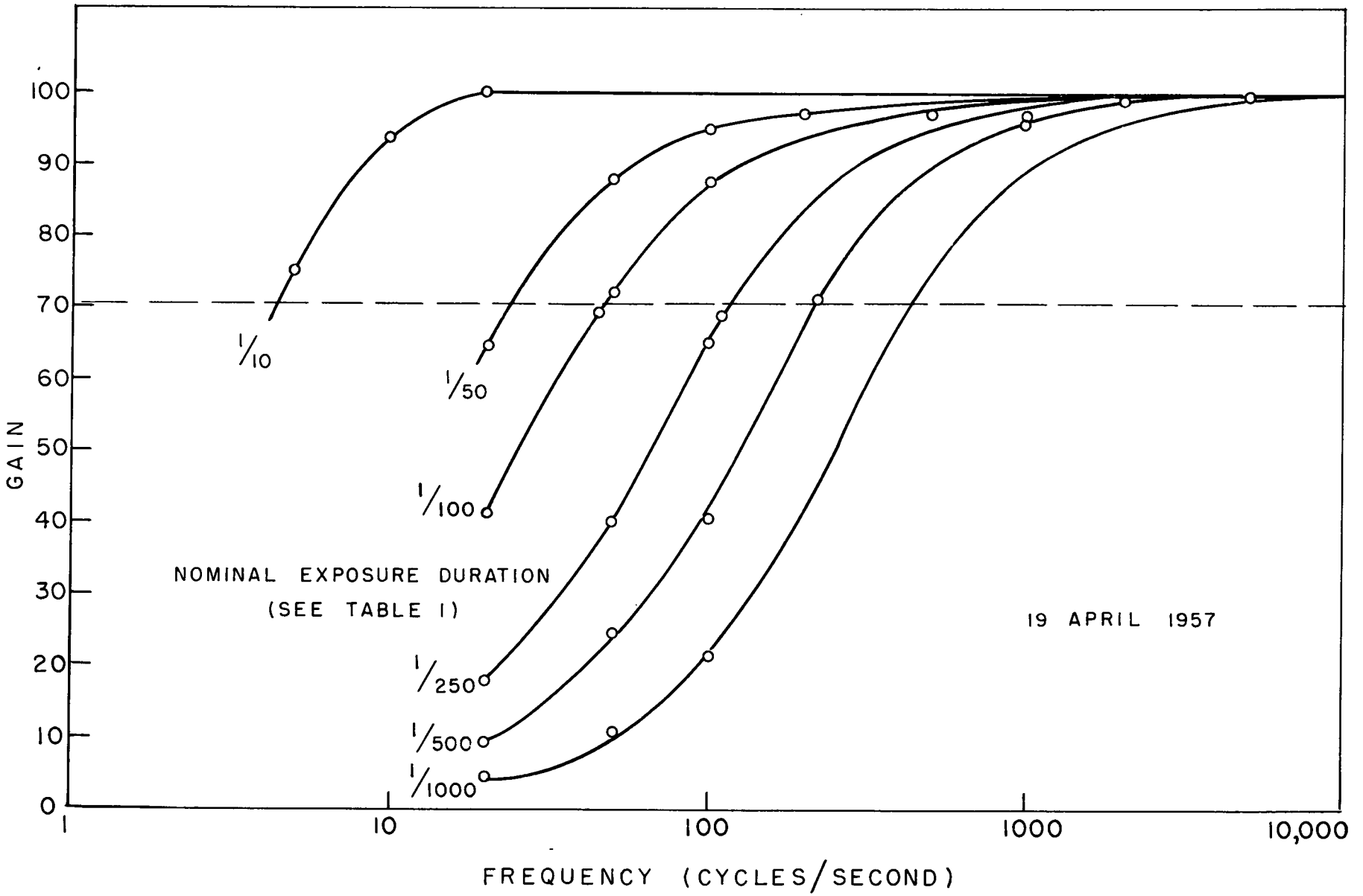
100
90
80
70
60
50
40
30
20
10
0
GAIN
1/10
1/50
1/100
1/250
1/500
1/1000
NOMINAL EXPOSURE DURATION
(SEE TABLE I)
19 APRIL 1957
1
10
100
1000
10,000
FREQUENCY (CYCLES/SECOND)

Fig. 7

switch was derived from these curves by noting their intersection with the 0.707 ordinate (dashed) line on Fig. 7 and setting this frequency equal to 0.446/T, in accordance with the equations developed on page 6 of Appendix B. The results of this procedure are given in Table 1.

Table 1

Nominal Exposure Interval (Seconds)	Corner Frequency (Cycles per Second)	Effective Exposure Interval (Seconds)
$\frac{1}{10}$ 0.1000	4.5	0.0991
$\frac{1}{50}$ 0.0200	24.0	0.0186
$\frac{1}{100}$ 0.0100	47.5	0.00940
$\frac{1}{250}$ 0.0040	116.	0.00385
$\frac{1}{500}$ 0.0020	210.	0.00212
$\frac{1}{1000}$ 0.0010	470.	0.00095

Performance of the Shimmer Meter Electronic System

Tests of the constancy of the multiplier phototube anode current for various dynode voltages showed the characteristics plotted in Fig. 8. This is an amazing constancy inasmuch as the dynode voltage range corresponds to more than 1000 to one in light level at the photocathode. The small residual variation in anode current was of marginal importance in its effect on the absolute magnitude of the signal indication of the instrument but was reflected in the noise output of the system. This was sometimes sufficient to require corrections to be made in the data. It was important, moreover, to restrict the light level at the photocathode by means of fixed filters attached to the phototube in order to keep the dynode voltage from having too high a value and producing, thereby, excess circuit noise. This is illustrated by Fig. 9, which shows measurements of rms noise output from the system for various dynode voltages. Typical operating conditions with one fixed neutral filter attached to the phototube are indicated by the vertical lines drawn through these curves. Ideally a variable density neutral filter should be used at the phototube in order that all measurements can be made at that dynode voltage which yields the smallest noise-and-ripple; from Fig. 9 this is seen to be approximately 475 volts. A servo-operated variable density neutral filter could have been incorporated in the instrument for this purpose.

Corrections of the data for noise can be made in terms of the curves in Fig. 9 if the dynode voltage is measured. A test point was provided on the chassis for connecting an external voltmeter for this purpose. It should be noted that the noise and signal currents combine as the square root of the sum of the squares of their separate values.

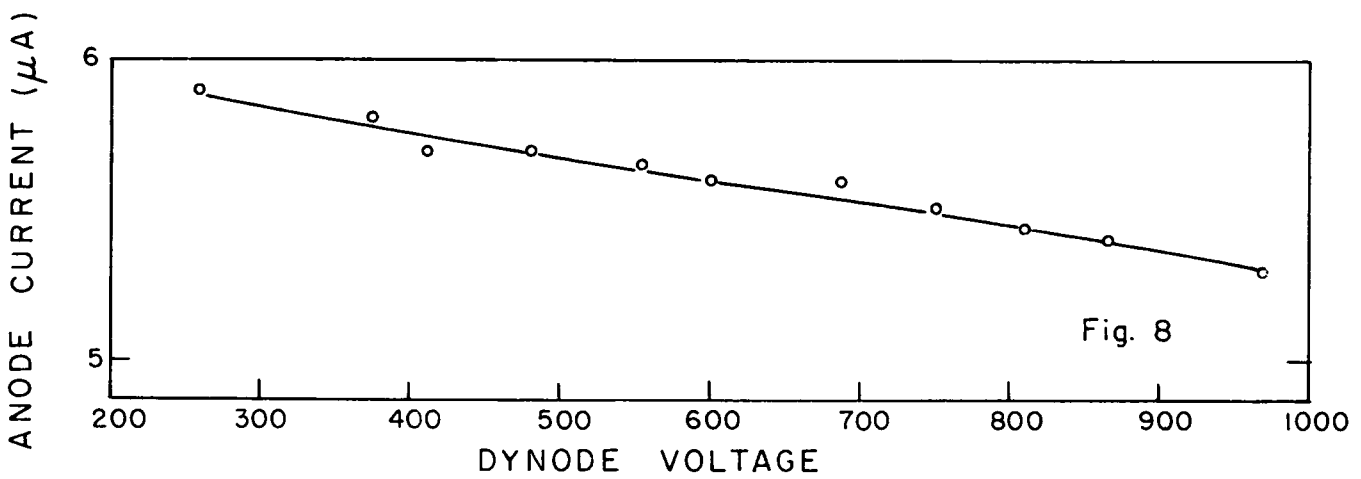
ANODE CURRENT (μA)
6
5
200
300
400
500
600
700
800
900
1000
DYNODE VOLTAGE
Fig. 8

Fig. 8

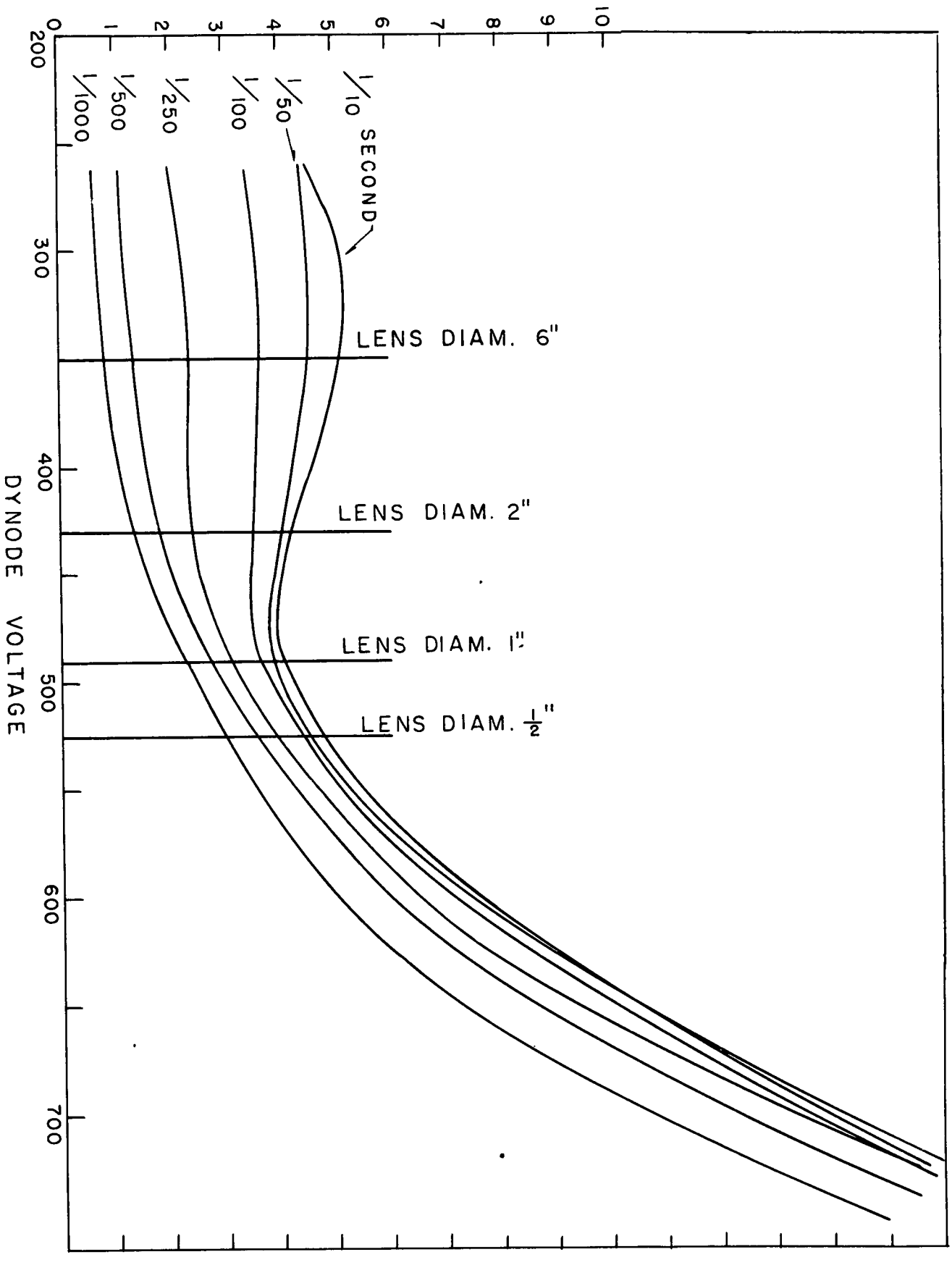
RMS NOISE OUTPUT (VOLTS)
0
1
2
3
4
5
6
7
8
9
10
200
300
400
500
600
700
DYNODE VOLTAGE
1/1000
1/500
1/250
1/100
1/50
1/10 SECOND
LENS DIAM. 6"
LENS DIAM. 2"
LENS DIAM. 1"
LENS DIAM. ½"

Fig. 9

Calibration of the Shimmer Meter

The shimmer meter measures root-mean-square modulation (M) of the light arriving at the photocathode of the multiplier phototube. This, in turn, depends upon the product of the rms deviation of image-forming rays (σ), the average fractional length of slit covered by the solar image (B), the angular length of the slits (slit length L divided by lens focal length F) and the square root of the number of slits used in the pattern N). Thus,

$$M = \sigma_{\infty}(z,\theta,\phi)/B\left(\frac{L}{F}\right)\sqrt{N}$$

From an electrical standpoint, the measured modulation is the ratio of the rms output voltage diminished by the gain of the amplifier to the average dc voltage across the load resistor of the multiplier phototube. Thus

$$M = \frac{V/G}{\bar{\ }}$$

where V is the rms voltage indicated by the thermal meter, G is the gain setting of the attenuator switch, I is the anode current of the multiplier phototube, and R is the resistance of the load resistor. Combining these two equations for rms modulation M and solving for $\sigma(z,\theta,\phi)$ there results

$$\sigma_{\infty}(z,\theta,\phi) = \frac{\frac{1}{\bar{\ }}}{}$$

In the experimental shimmer meter, the constants in the above equation had the following values:

$$\beta = 1/2$$

$$L = 0.1285 \text{ inches} \quad (L/F = 265 \text{ seconds of arc})$$

$$F = 100.0 \text{ inches}$$

$$N = 4$$

$$I = 5.70 \times 10^{-6} \text{ amperes, if the dynode voltage is 475 volts}$$

$$R = 20.0 \times 10^{6} \text{ ohms}$$

Thus,

$$\sigma_{\infty}(\lambda,\theta,\phi) = \frac{\frac{1}{2}(0.1285)(4)^{\frac{1}{2}} V}{(100.0)(5.70 \times 10^{-6})(20.0 \times 10^{6})G} = 1.13 \times 10^{-5} \frac{V}{G} \text{ radians}$$

or

$$\sigma_{\infty}(\lambda,\theta,\phi) = 2.3V/G \text{ seconds of arc.}$$

With skillful tracking of the sun, the shimmer meter could have been made direct reading by using slits 0.1285/2.32 = 0.0554" long, since then $\sigma_{\infty}(\lambda,\theta,\phi) = 1.00\ V/G$ seconds of arc.

It is interesting and significant that the calibration of the shimmer meter is entirely specified by its geometry and by measurable electrical circuit parameters. The calibration is valid, however, only if the motion of the image of the solar limb is completely correlated across the width of the slit. This requirement is examined analytically in Appendix C of this report.

EXPERIMENTS WITH THE SHIMMER METER

All of the data obtained with the shimmer meter were collected near Cape Kennedy, Florida, during the spring of 1957. The instrument was located at tracking camera stations along the beach overlooking the Atlantic Ocean. Figure 10 depicts a series of measurements on 20 March 1957. The rms deviation of image-forming rays associated with the solar image is seen to increase with exposure duration and to decrease as lens diameter is made progressively larger.

The effect of shimmer was less pronounced at the same location and at the same hour on the afternoon of 27 March 1957, as shown by Fig. 11. The same trends are seen in the data although the magnitudes of the readings were less.

APPLICATIONS OF SHIMMER METER DATA

The performance of diffraction limited telescopic systems in the presence of atmospheric boil is affected and controlled by both the soft and the hard components of shimmer as well as by diffraction. The instrument described in this report yields no information concerning the effects of soft shimmer, but this was believed, in 1957, to have negligible effect upon the uses to which tracking cameras were then being put. Optimization of telescope and camera aperture size under prevailing atmospheric conditions and assessment of the reward for reductions in exposure duration were among the envisioned applications of the instrument. It was intended also for use in selecting sites for large telescopes and cameras.

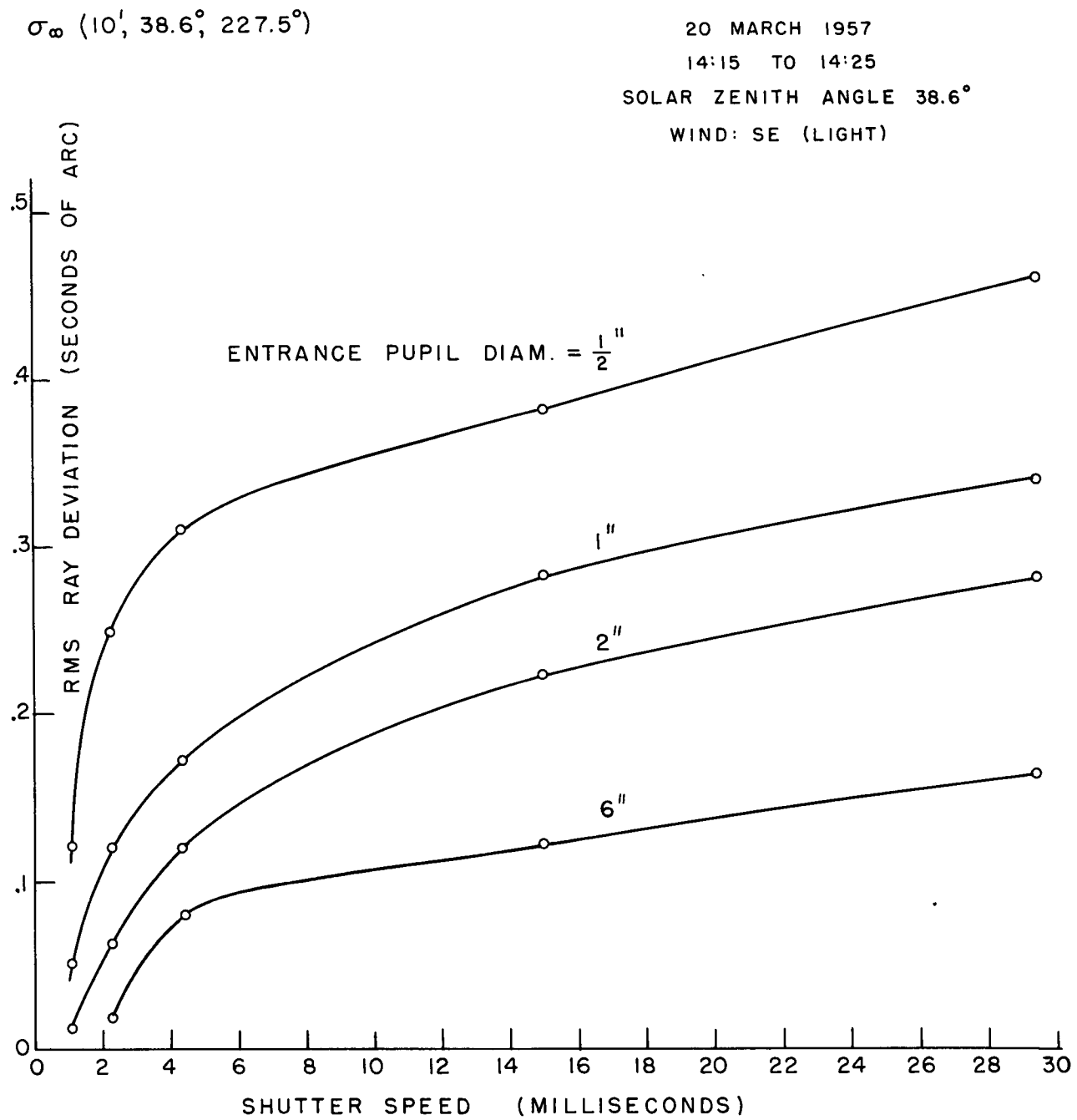
σ_∞ (10', 38.6°, 227.5°)
20 MARCH 1957
14:15 TO 14:25
SOLAR ZENITH ANGLE 38.6°
WIND: SE (LIGHT)
RMS RAY DEVIATION (SECONDS OF ARC)
ENTRANCE PUPIL DIAM. = 1/2"
1"
2"
6"
0
.1
.2
.3
.4
.5
0 2 4 6 8 10 12 14 16 18 20 22 24 26 28 30
SHUTTER SPEED (MILLISECONDS)

Fig. 10

27 MARCH 1957
14:05 TO 14:14
SOLAR ZENITH ANGLE 37.0°
WIND: NE (BRISK)
HIGH THIN CLOUDS

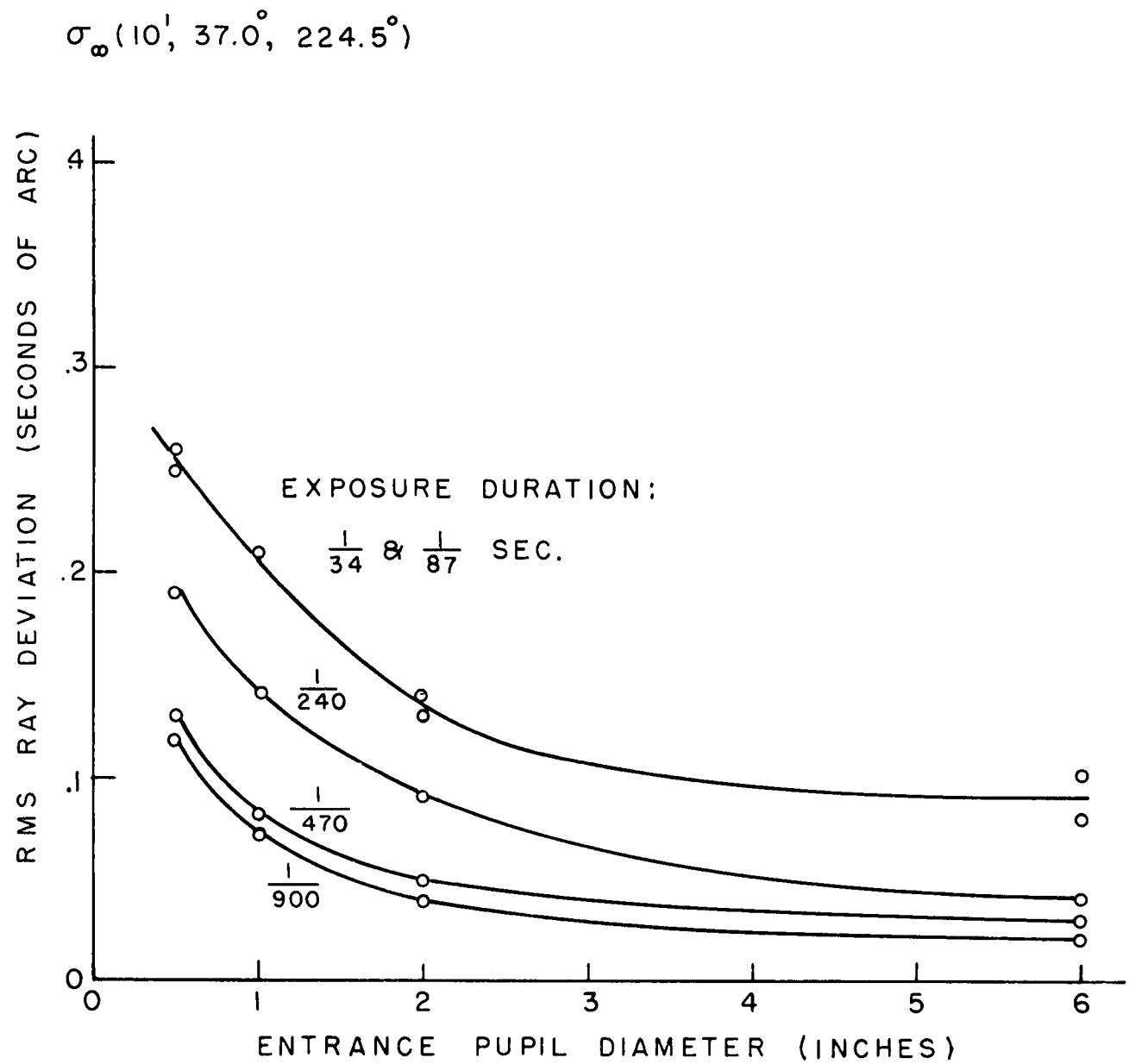

Fig. 11

Data from the shimmer meter, when combined with other measurable input information, were used to predict the limiting range to which telescopes and cameras could track aerial objects; this topic may be the subject of a subsequent report.

PRESENTATIONS

Demonstrations of the shimmer meter and presentations concerning its principles and the data secured with it were made to military and civilian personnel at the Air Force Missile Test Center, Patrick Air Force Base, Florida, during March and April 1957, at Eglin Air Force Base during May 1957, and at other times and places to representatives of the Air Force Cambridge Research Laboratory, the U. S. Naval Ordnance Test Station, the U. S. Navy Bureau of Ships, and other military agencies. Following these demonstrations and presentations the shimmer meter was dismantled. There has been no subsequent work on this topic by the Visibility Laboratory.

13 February 1957

SHIMMER METER CALIBRATION

J. L. Harris

Two cases will be considered. The first is the case of high angular correlation where the sun effectively moves as a unit.

The parameter, A, is the variance of a two dimensional normal distribution describing the frequency of the angular position of a point source. Sample values of interest supplied by Dr. Duntley are 0.2×10^{-8} sq. rad. to 1.4×10^{-8} sq. rad. This means the standard deviations range from $.447 \times 10^{-4}$ radians to 1.183×10^{-4} radians. In terms of minutes of arc

$$\sigma = .447 \times 10^{-4} \times 57.3 \times 60 = .1535 \text{ min.}$$

$$\sigma = 1.183 \times 10^{-4} \times 57.3 \times 60 = .407 \text{ min.}$$

The sun is approximately 30 minutes of arc. A slit which is 1 min. x 10 min. has a smaller dimension which is small compared to the 30 minutes. A rough scale might be as follows:

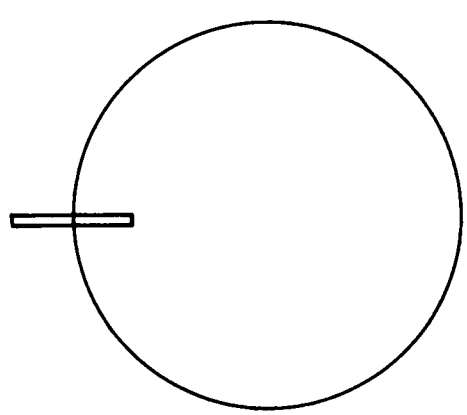

For the magnitudes of A, expected vertical movements of the sun will have nagligible effect on the flux variation as compared to the horizontal motion. For example, consider a vertical change of 2 minutes.

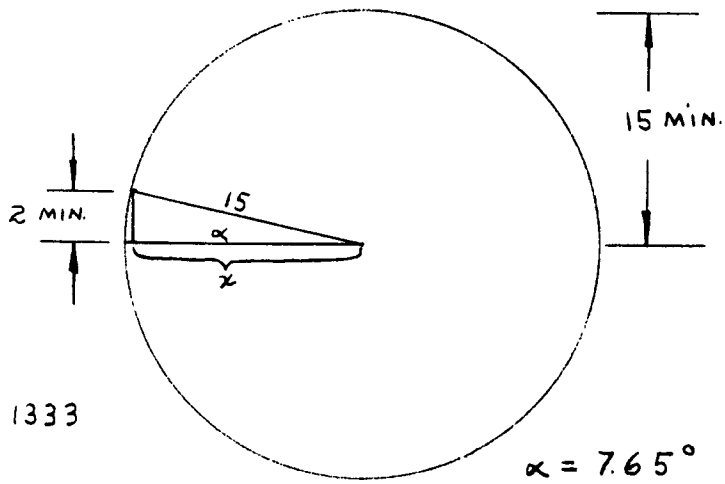

$\sin\alpha = \frac{2}{15} = .1333$

$\alpha = 7.65°$

$\tan\alpha = \frac{2}{\chi}$

$\chi = \frac{2}{\tan\alpha} = \frac{2}{.134} = 14.93$

The change in radius is .07 minutes. Thus the angular size of the filled portion of the slit is only changed by .07 minutes as compared to 2 minutes for a 2 minute horizontal shift. The ratio is

$$\frac{.07}{2} = .035 = 3.5\%$$

The approximation is therefore used that only horizontal motion need be considered.

The two dimensional normal distribution has the form

$$f(x,y) = \frac{1}{2\pi\sigma^2} e^{-\frac{x}{2\sigma^2}} e^{-\frac{y^2}{2\sigma^2}}$$

Where x and y are independent, as is assumed here, the distribution is a figure of revolution of the form

$$f(r) = K e^{-\frac{r^2}{2\sigma^2}}$$

where K is the normalizing constant. To find K the volume of the distribution must be equated to unity. Considering an incremental cylinder shell of radius r, thickness dr, height $K e^{-\frac{r^2}{2\sigma^2}}$ and circumference $2\pi R$, the incremental

volume is

$$dv = 2\pi r K e^{-\frac{r^2}{2\sigma^2}} dr$$

The total volume is

$$V = 2\pi K \int_0^\infty r e^{-\frac{r^2}{2\sigma^2}} dr$$

$$V = 2\pi K \left[-\sigma^2 e^{-\frac{r^2}{2\sigma^2}} \right]_0^\infty$$

$$V = 2\pi\sigma^2 K = 1$$

$$K = \frac{1}{2\pi\sigma^2}$$

Therefore

$$f(r) = \frac{1}{2\pi\sigma^2} e^{-\frac{r^2}{2\sigma^2}}$$

The variance of this distribution is

$$\sigma_r^2 = \int_0^\infty r^2 \cdot 2\pi r \cdot \frac{1}{2\pi\sigma^2} e^{-\frac{r^2}{2\sigma^2}} dr$$

$$\sigma_r^2 = \frac{1}{\sigma^2} \int_0^\infty r^3 e^{-\frac{r^2}{2\sigma^2}} dr$$

Let $u = r^2$ $\quad dv = r e^{-\frac{r^2}{2\sigma^2}}$

$du = 2r\,dr$ $\quad v = -\sigma^2 e^{-\frac{r^2}{2\sigma^2}}$

$$\sigma_r^2 = \frac{1}{\sigma^2}\left[-r^2\sigma^2 e^{-\frac{r^2}{2\sigma^2}} + \int \sigma^2 e^{-\frac{r^2}{2\sigma^2}} 2r\,dr \right]_0^\infty$$

$$\sigma_r^2 = \frac{1}{\sigma^2}\left[-r^2\sigma^2 e^{-\frac{r^2}{2\sigma^2}} + 2\sigma^4 \right]_0^\infty$$

$$\sigma_r^2 = \frac{1}{\sigma^2}\left[\lim_{r\to\infty} \frac{-\sigma^2 r^2}{e^{\frac{r^2}{2\sigma^2}}} + 2\sigma^4 \right]$$

$$\sigma_r^2 = \frac{2\sigma^4}{\sigma^4} = 2\sigma^2$$

$$\sigma_r = \sqrt{2}\,\sigma$$

Therefore the modulation will be a horizontal gaussian shift of the sun having a variance equal to $\frac{A}{2}$.

If the sun initially fills a fraction χ of the aperture then the d.c. flux will be proportional to $\chi \alpha_h$ where α_h is the horizontal angular subtense of the slit.

The percentage modulation is therefore

$$M = \frac{\sqrt{\frac{A}{2}}}{\chi \alpha_h}$$

This is the ratio of the rms fluctuation to the d.c. amplitude. In terms of the instrument readings

$$M = \frac{(\text{rms reading})}{(\text{gain for rms signal})\ (\text{d.c. reading})}$$

Equating the two equations and solving for A

$$A = 2\chi^2 \alpha_h^2 \quad \frac{(\text{rms reading - volts})^2}{(\text{gain})^2\ (\text{d.c. reading - volts})^2}$$

From the equation for M using the estimated values for A for a slit 1 min. X 10 min. (sun $\frac{1}{2}$ filling slit)

$$M = \frac{.1085}{.5 \times 10} = .0217 = 2.17\% \text{ or } \frac{.288}{.5 \times 10} = .0576 = 5.76\%$$

Note that a 10% error in allignment of edge of sun's disk means an error in A of

$$\epsilon = 100 \times \left[(1) - \left(\frac{.45}{.5}\right)^2\right] = 19\%$$

For the case of no angular correlation, let us first simplify the problem by assuming that we are considering a slit which is long compared to its height.

Here we need only consider the contribution to the variance due to vertical motion.

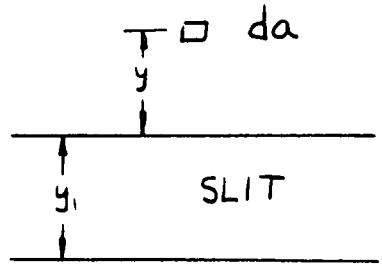

Consider an element da having an illuminance E. The flux from this element is $E\,da$. Over a period of time this elemental flux will be in the aperture a fractional time of

$$\frac{1}{\sqrt{2\pi}\,\sigma}\int_{y}^{y+y_1} e^{-\frac{y^2}{2\sigma^2}}\,dy$$

where is the standard deviation of the vertical normal distribution. A plot of flux through the aperture from the incremental area as a function of time might look as follows:

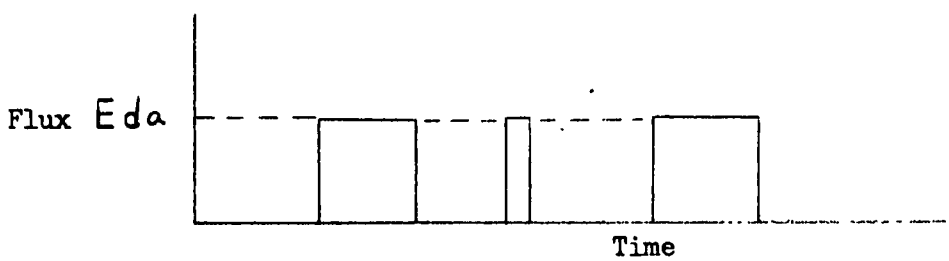

The incremental variance due to this incremental flux would be

$$d(\sigma^2) = \frac{1}{T}\int_0^T \overline{F(t)}^2\,dt - \overline{F}^2$$

where $\overline{F}$ is the average flux and is equal to

$$\overline{F} = \frac{1}{T}\int_0^T F(t)\,dt = E\,da\,\frac{1}{\sqrt{2\pi}\,\sigma}\int_{y}^{y+y_1} e^{-\frac{y^2}{2\sigma^2}}\,dy$$

For the first integral since the flux is either zero or $E\,da$, $(E\,da)^2$ may be factored from the integral and

$$d(\sigma^2) = (E\,da)^2\,\frac{1}{T}\int_0^{\gamma T} dt - (E\,da)^2\,\gamma^2$$

where $\Psi = \frac{1}{\sqrt{2\pi}\,\sigma} \int_{y}^{y+y_1} e^{-\frac{y^2}{2\sigma^2}}\, dy$

$$d(\sigma^2) = (E\,da)^2 [\Psi - \Psi^2]$$

Since Ψ is finite the total variance would be equal to zero because of the existence of the term $(da)^2$. Physically this is true because any statistics applied to the case of zero correlation means that we are treating a case where there exists an infinite number of independent actions and therefore we are sampling from an infinite population.

The shimmer meter can only be calibrated for the high correlation case unless the correlation is known. When so calibrated the value of A obtained represents a lower limit to the true value.

13 February 1957

FILTERING FOR THE SHIMMER METER

J. L. Harris

Consider the image of the sun's disk and aperture geometry as follows:

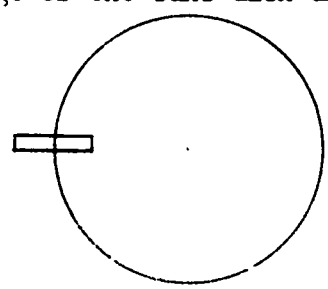

In the presence of shimmer the output from the photocell behind the disk will be modulated by the motion of the edge of the sun's disk within the aperture. The output from the photocell would be as follows:

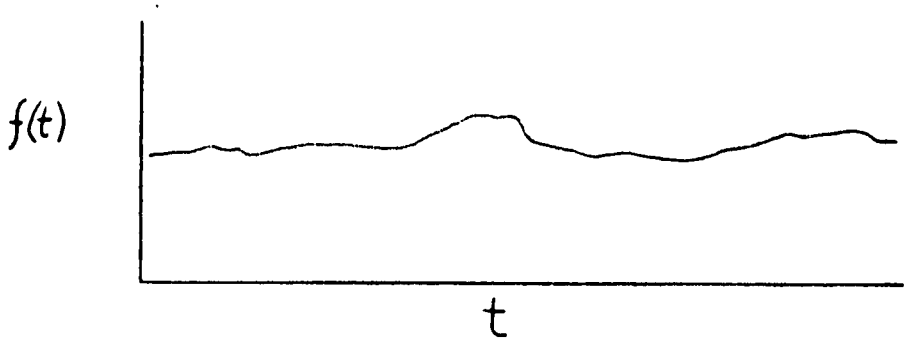

The camera would be examining and integrating an image over an exposure time, T. What we wish to know is for an integration period T, what will be the rms travel of the image. For any interval of length T there will be an average output from the photocell.

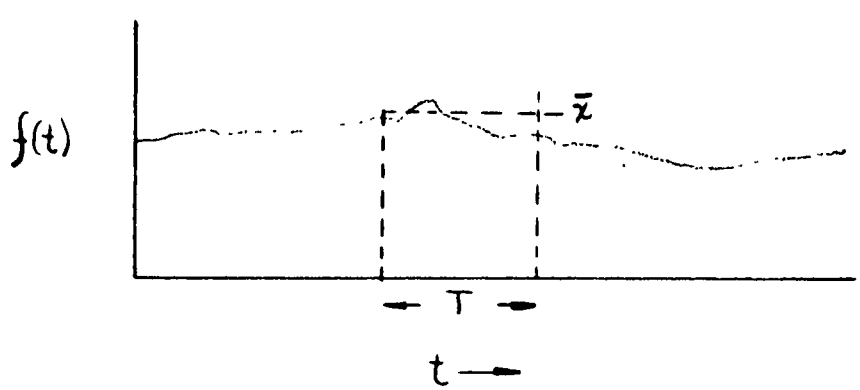

We wish to determine the rms value of the fluctuation about this average. The waveform $f(t)$ may be considered to consist of an infinite number of frequency components. By considering a component, ω , we can determine the filter which will allow us to perform the desired measurement. For the general case

$$e = E_\omega \sin(\omega t + \phi)$$

where ϕ is a random phase angle

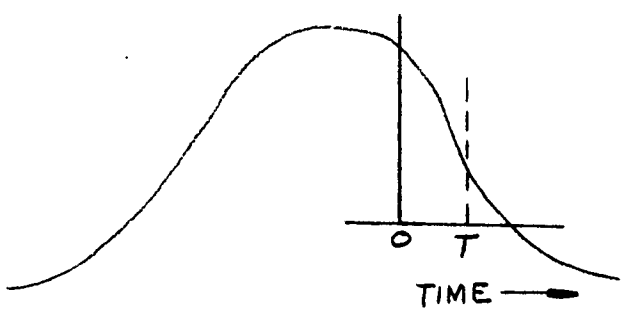

Each frequency component will, in general, contribute to the d.c. level over the time interval T. Since we are only interested in the fluctuations about the mean we must first find the average value of the component over the time interval T.

$$\bar{x} = \frac{E_\omega}{T_o}\int_o^T \sin(\omega t + \phi)\,dt$$

$$\bar{x} = \frac{E_\omega}{T}\left[\frac{-\cos(\omega t + \phi)}{\omega}\right]_o^T$$

$$\bar{x} = \frac{E_\omega}{\omega T}\left[\cos\phi - \cos(\omega T + \phi)\right]$$

We are interested in σ, the rms fluctuation about the mean. This may be found as

$$\sigma^2 = \frac{1}{T}\int_o^T \left\{E_\omega \sin(\omega t + \phi) - \frac{E_\omega}{\omega T}\left[\cos\phi - \cos(\omega T + \phi)\right]\right\}^2 dt$$

$$\sigma^2 = \frac{1}{T}\int_0^T E_\omega^2 \sin^2(\omega t+\phi)\,dt \quad \leftarrow A$$

$$- \frac{1}{T}\int_0^T \frac{2E_\omega^2}{\omega T}\sin(\omega t+\phi)\left[\cos\phi - \cos(\omega T+\phi)\right]dt \quad \leftarrow B$$

$$+ \frac{1}{T}\int_0^T \frac{E_\omega^2}{\omega^2 T^2}\left[\cos\phi - \cos(\omega T+\phi)\right]^2 dt \quad \leftarrow C$$

$$A = \frac{1}{T}\int_0^T E_\omega^2 \sin^2(\omega t+\phi)\,dt$$

$$A = \frac{E_\omega^2}{T}\int_0^T \sin^2(\omega t+\phi)\,dt$$

$$A = \frac{E_\omega^2}{T}\int_0^T \left[\frac{1}{2} - \frac{1}{2}\cos^2(\omega t+\phi)\right]dt$$

$$A = \frac{E_\omega^2}{T}\left[\frac{t}{2} - \frac{1}{2}\,\frac{\sin^2(\omega t+\phi)}{2\omega}\right]_0^T$$

$$A = \frac{E_\omega^2}{T}\left[\frac{T}{2} - \frac{\sin 2(\omega T+\phi)}{4\omega} + \frac{\sin 2\phi}{4\omega}\right]$$

Since ϕ is random we must average over all ϕ's

$$\bar{A} = \frac{1}{2\pi}\int_0^{2\pi} A\,d\phi = \frac{E_\omega^2}{2}$$

$$B = -\frac{1}{T}\int_0^T \frac{2E_\omega^2}{\omega T}\sin(\omega t+\phi)\left[\cos(\omega T+\phi)\right]dt$$

$$B = -\frac{2E_\omega^2}{\omega T^2}\left[\cos\phi - \cos(\omega T+\phi)\right]\int_0^T \sin(\omega t+\phi)\,dt$$

$$B = -\frac{2E_\omega^2}{\omega T^2}\left[\cos\phi - \cos(\omega T+\phi)\right]\left[-\frac{\cos(\omega t+\phi)}{\omega}\right]_0^T$$

$$B = -\frac{2E_\omega^2}{\omega^2 T^2}\left[\cos\phi - \cos(\omega T+\phi)\right]\left[\cos\phi - \cos(\omega T+\phi)\right]$$

$$B = -\frac{2E_\omega^2}{\omega^2 T^2}\left[\cos\phi - \cos(\omega T+\phi)\right]^2$$

Averaging with respect to ϕ

$$\bar{B} = -\frac{2E_\omega^2}{\omega^2 T^2}\left\{\frac{1}{2\pi}\int_0^{2\pi}\cos^2\phi\, d\phi - \frac{2}{2\pi}\int_0^{2\pi}\cos\phi\cos(\omega T+\phi)d\phi + \frac{1}{2\pi}\int_0^{2\pi}\cos^2(\omega T+\phi)\, d\phi\right\}$$

$$\bar{B} = -\frac{2E_\omega^2}{\omega^2 T^2}\left\{\frac{1}{2\pi}\int_0^{2\pi}\left(\frac{1}{2}+\frac{1}{2}\cos 2\phi\right)d\phi - \frac{2}{2\pi}\int_0^{2\pi}\cos^2\phi\cos\omega T d\phi + \frac{2}{2\pi}\int_0^{2\pi}\cos\phi\sin\phi\sin\omega T d\phi + \frac{1}{2\pi}\int_0^{2\pi}\left[\frac{1}{2}+\frac{1}{2}\cos 2(\omega T+\phi)\right]d\phi\right.$$

$$\bar{B} = -\frac{2E_\omega^2}{\omega^2 T^2}\left[\frac{1}{2} - \frac{2\cos\omega T}{2\pi}\int_0^{2\pi}\left(\frac{1}{2}+\frac{1}{2}\cos 2\phi\right)d\phi + \frac{2\sin\omega T}{2\pi}\sin^2\phi\Big|_0^{2\pi} + \frac{1}{2}\right]$$

$$\bar{B} = -\frac{2E_\omega^2}{\omega^2 T^2}\left[1-\cos\omega T\right]$$

$$\bar{B} = -\frac{2E_\omega^2}{\omega^2 T^2}\,2\sin^2\left(\frac{\omega T}{2}\right) = -E_\omega^2\,\frac{\sin^2\left(\frac{\omega T}{2}\right)}{\left(\frac{\omega T}{2}\right)}$$

$$C = \frac{1}{T}\int_0^T \frac{E_\omega^2}{\omega^2 T^2}\left[\cos\phi - \cos(\omega T+\phi)\right]^2 dt$$

$$C = \frac{E\omega^2}{\omega^2 T^2}\left[\cos\phi - \cos(\omega T + \phi)\right]^2$$

Since it may now be seen that

$$C = -\frac{1}{2}B$$

then

$$\bar{C} = +\frac{E_\omega^2}{2}\,\frac{\sin\left(\frac{\omega T}{2}\right)}{\left(\frac{\omega T}{2}\right)^2}$$

Combining A, B and C

$$\sigma^2 = \frac{E_\omega^2}{2} - E_\omega^2\left[\frac{\sin^2\left(\frac{\omega T}{2}\right)}{\left(\frac{\omega T}{2}\right)^2}\right] + \frac{E_\omega^2}{2}\left[\frac{\sin^2\left(\frac{\omega T}{2}\right)}{\left(\frac{\omega T}{2}\right)^2}\right]$$

$$\sigma^2 = \frac{E_\omega^2}{2}\left[1 - \frac{\sin^2\left(\frac{\omega T}{2}\right)}{\left(\frac{\omega T}{2}\right)^2}\right]$$

and

$$\sigma = \frac{E_\omega}{\sqrt{2}}\left[1 - \frac{\sin^2\left(\frac{\omega T}{2}\right)}{\left(\frac{\omega T}{2}\right)^2}\right]^{1/2}$$

Notice that $\frac{E\omega}{\sqrt{2}}$ is the true rms value of the frequency component being considered. If this component were passed without attenuation we would measure it as $\frac{E_\omega}{\sqrt{2}}$. The equation tells us, however, that to get the desired measurement we must weight this frequency component with a filter having an amplitude characteristic

$$A = \left[1 - \frac{\sin^2\left(\frac{\omega T}{2}\right)}{\left(\frac{\omega T}{2}\right)^2}\right]^{1/2}$$

The attached graph shows a plot of this function. The highpass RC circuit

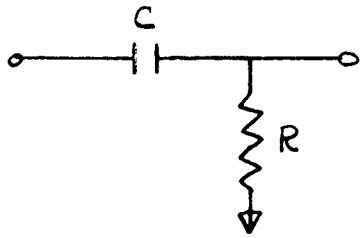

has a transfer function

$$\left|\frac{E_{OUT}}{E_{IN}}\right| = \frac{\omega RC}{\sqrt{\omega^2(RC)^2+1}}$$

The 3 db point of the RC filter occurs where

$$\left|\frac{E_{OUT}}{E_{IN}}\right| = 0.707 = \frac{\omega_{1/2} RC}{\sqrt{\omega_{1/2}^2(RC)^2+1}}$$

$$\omega_{1/2}^2(RC)^2+1 = 2\,\omega_{1/2}^2(RC)^2$$

$$\omega_{1/2}^2(RC)^2 = 1$$

$$\omega_{1/2} = \frac{1}{RC}$$

From the plot of $\left[1 - \frac{\sin^2\left(\frac{\omega T}{2}\right)}{\left(\frac{\omega T}{2}\right)^2}\right]^{1/2}$

the half power point appears to occur when

$$\frac{\omega T}{2} \doteq 1.4$$

or

$$\omega_{1/2} = \frac{2.8}{T}$$

Matching the two functions at the half power point then

$$\frac{1}{RC} = \frac{2.8}{T}$$

or

$$RC = \frac{T}{2.8} = 0.357\,T$$

This is the value of RC which would be selected to approximate the correct filter characteristic. Since

$$\left|\frac{E_{OUT}}{E_{IN}}\right| = \frac{\omega RC}{\sqrt{\omega^2(RC)^2+1}}$$

$$\left|\frac{E_{OUT}}{E_{IN}}\right| = \frac{0.357\,\omega T}{\sqrt{.128\,\omega^2 T^2+1}}$$

$\frac{\omega T}{2}$	ωT	$0.357\omega T$	$(0.357\omega T)^2$	$(0.357\omega T)^2+1$	$\sqrt{\quad}$	$\left\|\frac{E_{OUT}}{E_{IN}}\right\|$
0	0	0	0	1.0	1.0	0
1	2	0.714	0.51	1.51	1.23	0.58
2	4	1.428	2.04	3.04	1.745	0.818
3	6	2.142	4.6	5.6	2.37	0.905
4	8	2.856	8.12	9.12	3.02	0.945
5	10	3.570	12.7	13.7	3.7	0.965

The match is quite good. The maximum error of 10% would only exist if the shimmer frequencies were concentrated at

$$\frac{\omega T}{2} = 3 \quad \text{OR} \quad \omega = \frac{6}{T}$$

The measurement could be made as follows:

1. Depending on the amplitude of the expected fluctuations some amplification will be required. The low frequency response of this amplification must be good enough so that the frequency response of the system will be determined by the RC filter only.
2. An RC highpass filter may be placed in the circuit at any stage of the amplification. This could be either fixed RC's with a

switch, each RC corresponding to a desired exposure time T or a fixed C, variable R calibrated in terms of T.

3. A low pass filter passing only that portion of the spectrum where shimmer is expected should be inserted. This will serve to minimize shot noise.

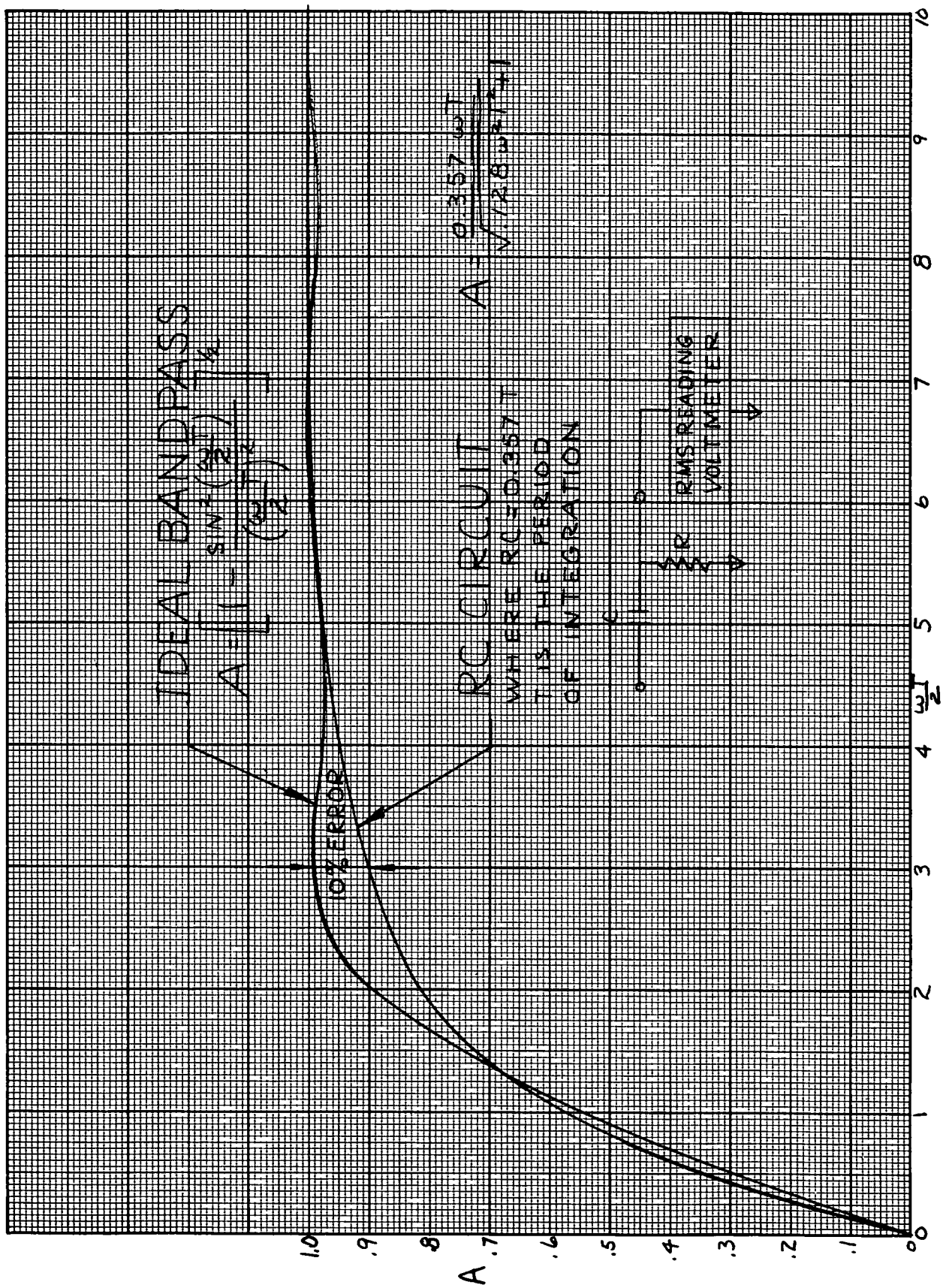
IDEAL BANDPASS
REQUIRED WHERE PC = 0.357
WITH 3 TIME PERIOD OF INTEGRATION
0% ERROR
RMS READING VOLTMETER
A
0.357
1/√28
A
1.0
.9
.8
.7
.6
.5
.4
.3
.2
.1
0
1
2
3
4
5
6
7
8
9
10
3 1/2

UNCLASSIFIED
Security Classification

DOCUMENT CONTROL DATA - R&D
(Security classification of title, body of abstract and indexing annotation must be entered when the overall report is classified)

1. ORIGINATING ACTIVITY (Corporate author)	2a. REPORT SECURITY CLASSIFICATION
Visibility Laboratory University of California San Diego, California 92152	UNCLASSIFIED 2b. GROUP

3. REPORT TITLE

AN APPARATUS FOR THE MEASUREMENT OF AN EFFECT OF ATMOSPHERIC BOIL (The Shimmer Meter)

4. DESCRIPTIVE NOTES (Type of report and inclusive dates)

Final Report

5. AUTHOR(S) (Last name, first name, initial)

Duntley, Seibert Q., Harris, James L., and Austin, Roswell W.

6. REPORT DATE	7a. TOTAL NO. OF PAGES	7b. NO. OF REFS
May 1968	43	3

8a. CONTRACT OR GRANT NO.	9a. ORIGINATOR'S REPORT NUMBER(S)
NObs-84075 b. PROJECT NO.	SIO Ref. 68-15
c. Assignment 9 d.	9b. OTHER REPORT NO(S) (Any other numbers that may be assigned this report)

10. AVAILABILITY/LIMITATION NOTICES

Distribution of this document is unlimited.

11. SUPPLEMENTARY NOTES	12. SPONSORING MILITARY ACTIVITY
	Naval Ship Systems Command Department of the Navy Washington, D. C. 20360

13. ABSTRACT

This report presents a method for the measurement of an effect of atmospheric boil in terms of the root-mean square deviation of the image-forming rays that contribute to the reproduction of fine detail, and describes an experimental (breadboard) version of an instrument near Cape Kennedy, Florida is presented. The effect of refractive inhomogeneities in the atmosphere (boil) on image quality is described in terms of the variance of a two-dimensional normal distribution describing the frequency of the apparent angular position of object points.

DD FORM 1 JAN 64 1473

UNCLASSIFIED
Security Classification

14 KEY WORDS	LINK A		LINK B		LINK C	
	ROLE	WT	ROLE	WT	ROLE	WT
Shimmer						
Boil						
Atmospheric Optics						
Tracking Cameras						
Telescopes						